

A Photoelectron–Photoion Coincidence Study of the ICH₂CN Ion Dissociation: Thermochemistry of •CH₂CN, ⁺CH₂CN, and ICH₂CN

Rick D. Laflaur, Balint Szatary,[†] and Tomas Baer*

Department of Chemistry, University of North Carolina, Chapel Hill, North Carolina 27599-3290

Received: October 6, 1999; In Final Form: December 13, 1999

The dissociation energies and dissociation dynamics of iodoacetonitrile (ICH₂CN) have been investigated by the photoelectron photoion coincidence (PEPICO) spectroscopy technique. The 0 K onsets for the following products were determined: ⁺CH₂CN + I• (12.188 ± 0.005 eV) and •CH₂CN + I⁺ (12.345 ± 0.010 eV). From the difference between these two values the ionization energy of the •CH₂CN was found to be 10.294 ± 0.010 eV. By using a thermodynamic cycle that involves the gas phase acidity of CH₃CN, the electron affinity of the •CH₂CN radical, and an accurate heat of formation of acetonitrile, a Δ_fH°₂₉₈(ICH₂CN) of 172.5 ± 4.0 kJ mol⁻¹ is derived. This latter value is considerably higher than the best theoretical value of 153 kJ mol⁻¹.

Introduction

The thermochemistry of free radicals and their closed-shell anions and cations can be investigated by several routes. Because each method has its pitfalls, it is highly advantageous to approach a problem from as many experimental routes as seems feasible.¹ The •CH₂CN system is one that can be investigated by multiple routes. For instance, the bond dissociation energy of acetonitrile (CH₃CN) yields the heat of formation of the •CH₂CN radical if the heat of formation of the starting compound is known (which it is in this case). In addition, the gas phase acidity of acetonitrile leads to a heat of formation of ⁻CH₂CN through the reaction CH₃CN → ⁻CH₂CN + H⁺. When this value is combined with the electron affinity for •CH₂CN, the heat of formation of •CH₂CN can be derived. This approach is totally independent of the thermal neutral dissociation kinetics approach in which the bond energies are directly measured from the activation energy of the fragmentation reaction. A final method involves dissociative photoionization of a compound such as XCH₂CN → ⁺CH₂CN + X•. When this onset is combined with the measured ionization energy of the free radical, •CH₂CN, we have a third method for determining the heat of formation of the free radical. Ultimately, all of these methods must agree. In addition, they should agree with theoretical calculations of these same quantities.

In a recent publication, Mayer et al.² reported on the thermochemistry of CH₃CN, ⁻CH₂CN, •CH₂CN, ⁺CH₂CN, and two of their isomers using high-level ab initio MO methods including G2^{3,4} to evaluate their structures and energies. In addition, they calculated the heat of formation of the ICH₂CN molecule. More recently, Lau et al.,⁵ using a G2 approach that incorporated an energy correction for spin contamination, reported calculations on about 10 isomers of C₂H₂N free radicals and their cationic species. The results were compared to those obtained from the available experiments. While the agreement was moderately good for some of the species, the calculations by Mayer et al.² were in glaring disagreement with the experimental results for the dissociative ionization of the ICH₂-

CN molecule. Holmes and Mayer⁶ had measured the onset for the ⁺CH₂CN + I• channel. By estimating a heat of formation of the parent iodoacetonitrile using group substitution methods, they arrived at a ⁺CH₂CN heat of formation which differed from one derived by the other cycles by as much as 30 kJ mol⁻¹, which is beyond the claimed accuracy (about ±12 kJ mol⁻¹) of either method. In their theoretical paper on this system, Mayer et al.² confirmed the ICH₂CN heat of formation assumed by Holmes and Mayer. Thus, either the Δ_fH°(ICH₂CN) is wrong or the dissociation products are not the ones expected.

Experimental methods suffer from the fact that the measurements of onsets or equilibrium constants provide little information about the structure of the species produced. Thus, considerable efforts are expended in establishing structures of the species under study. For instance, if in the acid equilibrium study the acetonitrile were to rearrange to give an anion with a structure other than ⁻CH₂CN (e.g., ⁻CH₂NC), then errors could be introduced. It turns out that the ⁻CH₂CN ion structure is the most stable one, so this is not a problem in this reaction. On the other hand, among the cations, the ⁺CH₂CN ion is not the most stable structure. The cyclic ion in which each carbon atom is bonded to a hydrogen atom is 12–16 kJ mol⁻¹ more stable than the “linear” CH₂CN⁺ isomer. According to both sets of ab initio calculations,^{2,5} the H₂CCN⁺ ion structure is the second most stable form. The third most stable ion has the CH₂NC⁺ structure and lies some 20–30 kJ/mol higher in energy. Rearrangement of fragment ions in the course of dissociation is commonplace.^{7,8} In fact, we have established that in the case of BrCH₂CN, the cyclic product ion is formed at the dissociation threshold.⁹ Because the experimentally derived heat of formation of ICH₂CN is greater than the calculated ab initio value, the formation of the cyclic ⁺CH₂CN ion in the dissociative photoionization would in fact account for this discrepancy in the heat of formation of iodoacetonitrile.

What is the evidence that the “linear” ⁺CH₂CN ion is produced from the dissociative ionization of iodoacetonitrile? Holmes and Mayer⁶ conducted kinetic energy release experiments on the reaction



[†] Present address: Department of General and Inorganic Chemistry, Eotvos Lorand University, Budapest, Hungary.

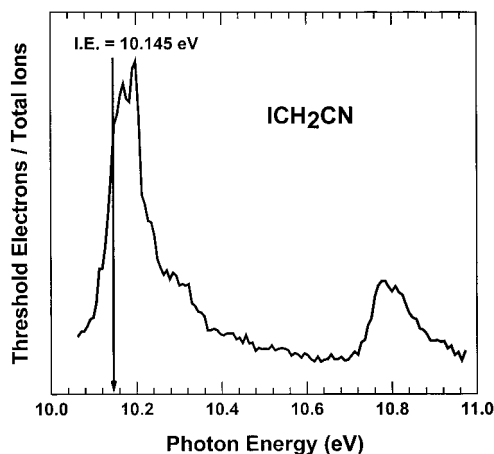


Figure 1. Threshold photoelectron spectrum of ICH_2CN in the vicinity of its ionization energy. The two peaks correspond to the ground electronic state and its spin-orbit component.

and determined that the dissociative loss of iodine from $\text{ICH}_2\text{CN}^{*+}$ is not accompanied by a release of kinetic energy so that this reaction does not proceed over a potential energy barrier. Furthermore, the results of collision-induced dissociation experiments on the product $^+\text{CH}_2\text{CN}$ ion strongly suggested that the “linear” form is produced in this reaction.

The current study probes this and other discrepancies through a detailed investigation of the thermochemistry of ICH_2CN , $^+\text{CH}_2\text{CN}$, and $\cdot\text{CH}_2\text{CN}$. Threshold photoelectron-photoion coincidence (PEPICO) experiments have been conducted on iodoacetonitrile in order to determine an accurate dissociative photoionization onset and also to determine if the “linear” form of the $^+\text{CH}_2\text{CN}$ cation could be confirmed. An obvious shortcoming of the previous determination of the dissociation onset¹⁰ was the lack of information about the dissociation rate. Such rates can be measured by PEPICO by modeling the metastable decay of the $^+\text{CH}_2\text{CN}$ with the statistical RRKM theory. It is also possible to account for the kinetic shift in the observed onset, which is due to the possibility of slow decay rates at the dissociation threshold.^{11,12}

Experimental Approach

The experimental details and operating principles of the threshold photoelectron-photoion coincidence, TPEPICO, technique have been discussed in earlier publications.^{13,14} Briefly, ions are generated by dispersed radiation from a 1m normal incidence monochromator with a resolution of 2 Å (17 meV at 10 eV photon energy). Ions and electrons are extracted in opposite directions by an electric field of 20 V/cm. Threshold electrons pass through a 10 cm pipe with small apertures followed by a hemispherical electrostatic energy analyzer. The resolution for the threshold electrons is about 30 meV. Ions are extracted via two stages of acceleration and pass through a 30 cm drift region with an energy of 220 V. The extraction voltages were adjusted to conform to the Wiley and McLaren space focusing conditions.¹⁵ Ion time-of-flight (TOF) distributions are obtained by using the electrons as start and the ions as stop signals.

When ions dissociate slowly in the acceleration region, their TOF distribution is asymmetric. The analysis of this distribution provides information about the dissociation rates which can be used to determine accurate onsets for dissociation by extrapolating the measured dissociation rates to their minimum value at the dissociation threshold. Iodoacetonitrile vapor (98% purity, Aldrich Chemical Co. Inc.) was introduced into the ionization

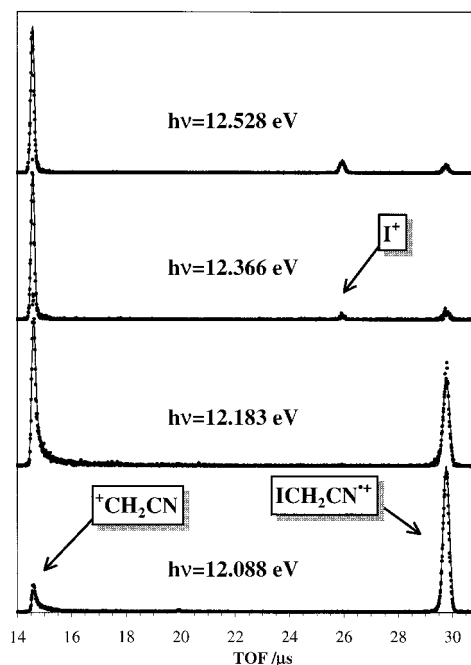


Figure 2. Some representative time-of-flight distributions at several photon energies. The slight asymmetry in the low-energy data is a result of the slow dissociation. The solid lines are calculated TOF distributions assuming an RRKM rate constant shown in Figure 5 and the energy function shown in Figure 4.

region through a needle pointing into the ionization region. Ions exiting the 32 cm drift tube were detected with an impedance matched set of microchannel plates. The amplified electron and ion signals were sent to a discriminator and time-to-pulse height converter, the output of which was passed to a multichannel analyzer where the number of coincidence events were recorded as a function of their time of flight.

Results and Discussion

Although the ionization energies of fluoroacetonitrile, chloroacetonitrile, and bromoacetonitrile are well-known, the IE of iodoacetonitrile has not been published. Figure 1 shows the threshold photoelectron spectrum (TPES) from 10.0 to 11.0 eV. The adiabatic ionization energy, determined to be 10.145 ± 0.010 eV, corresponds to the removal of one of the lone pair electrons from the I atom. This value was chosen on the basis of a similar TPES spectrum of CH_3I whose IE is well-known. In addition, the inflection point of the PIE scan was another criterion for assigning the IE as 10.145 eV. The spectrum also shows the excited state at 10.760 eV which corresponds to the higher spin-orbit state. Typical coincidence TOF mass spectra of iodoacetonitrile recorded at 298 K and at several photon energies are illustrated in Figure 2. The spectra show features associated with the iodoacetonitrile radical cation, $\text{ICH}_2\text{CN}^{*+}$, at low photon energies, and $^+\text{CH}_2\text{CN}$ and I^+ at higher photon energies. The asymmetric shape of the $^+\text{CH}_2\text{CN}$ peak at 12.088 and 12.183 eV is attributed to the metastable decay of $\text{ICH}_2\text{CN}^{*+}$ within the acceleration region of the spectrometer, and hence the arrival times of $^+\text{CH}_2\text{CN}$ at the ion detector are spread out over a small range of flight times. The rate constants for the decay of $\text{ICH}_2\text{CN}^{*+}$ were extracted from the data by modeling the asymmetric portion of the $^+\text{CH}_2\text{CN}$ peak. The solid lines passing through the data points were calculated based on an assumed $k(E)$ rate curve. The metastable region extends only over a range of about 0.1 eV. At higher energy all fragment ion peaks are symmetric. Figure 3 is a breakdown diagram that

TABLE 1: Vibrational Frequencies of the $\text{ICH}_2\text{CN}^{+\bullet}$ Ion and the Two Transition States

ion	vibrational frequencies ^a											
$\text{ICH}_2\text{CN}^{+\bullet}$	2991	2970	2316	1283	1205	1130	995	565	419	339	317	147
TS1	2991	2970	2316	1350	1160	1060	1046	299	118	89	80	
TS2	3121	3090	2626	1341	1051	1000	560	433	121	90	62	

^a The $\text{ICH}_2\text{CN}^{+\bullet}$ frequencies are calculated by ab initio MP2 methods, while the transition state frequencies for the $\text{CH}_2\text{CN}^{+\bullet}$ channel (TS1) and the $\text{I}^{+\bullet}$ channel (TS2) were varied to obtain a fit to the data.

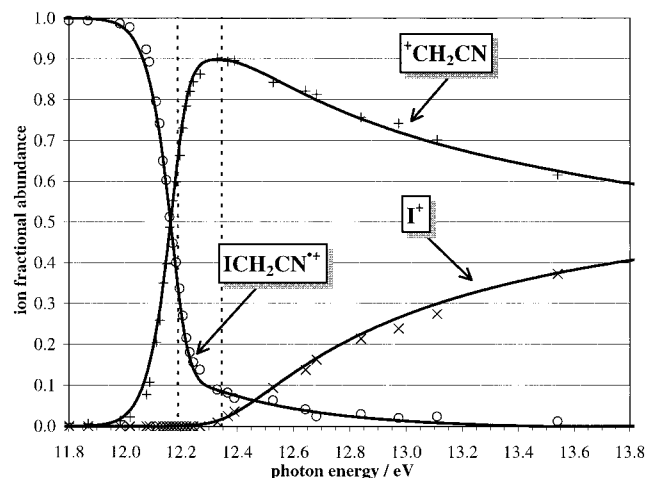


Figure 3. Breakdown diagram of the $\text{ICH}_2\text{CN}^{+\bullet}$ ion from threshold up to 13 eV. The dashed lines indicate the 0 K dissociation limits determined by modeling the dissociation dynamics with the RRKM theory, the thermal energy distribution of ICH_2CN , and the analyzer function of our PEPICO apparatus.

illustrates the fractional abundances of $\text{ICH}_2\text{CN}^{+\bullet}$, $^+\text{CH}_2\text{CN}$, and $\text{I}^{+\bullet}$ as a function of photon energy. It is evident that the lowest energy dissociation leads to $^+\text{CH}_2\text{CN}$ (I^{\bullet} atom loss) while at higher energies, the $\text{I}^{+\bullet}$ ($^+\text{CH}_2\text{CN}$ loss) channel becomes significant. The solid lines through the data points were obtained by modeling the dissociation rates using the RRKM statistical theory as well as the thermal energy distribution of ICH_2CN , as discussed below.

The form of the microcanonical energy dependent rate constant, $k(E)$, for a unimolecular reaction in accordance with the RRKM statistical theory¹⁶ is shown in eq 2

$$k(E) = \frac{\sigma N^{\ddagger}(E-E_0)}{h\rho(E)} \quad (2)$$

in which σ is the reaction symmetry factor which is one in this case, $N^{\ddagger}(E-E_0)$ is the sum of states of the transition state from the threshold energy E_0 (the barrier height) to the total energy E , $\rho(E)$ is the density of states, and h is Planck's constant. The density and sum of states were calculated using the vibrational frequencies (shown in Table 1) of the parent ion and the corresponding transition states. The parent ion vibrational frequencies were obtained from ab initio molecular orbital calculations (MP2) using the Gaussian 94 suite of programs.¹⁷ The threshold energy of activation and transition state vibrational frequencies were fitting parameters in the RRKM equation. The dissociation onset is thus derived from the extrapolation of the $k(E)$ curve to the dissociation onsets. This approach ensures that the derived onsets are not shifted to higher energies by the kinetic shift.

The data were analyzed by simultaneously fitting the asymmetric TOF distributions at various photon energies and the breakdown diagram. The fitting procedure took into account the thermal energy distribution of ICH_2CN , the resolution of the light source monochromator, and the analyzer function for

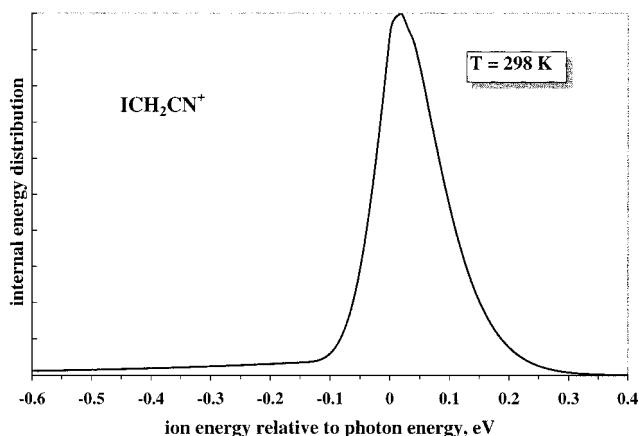


Figure 4. Energy function used to model both the breakdown diagram and the TOF distributions. The long tail to the low-energy side is a result of “hot” electrons passing through our analyzer, while the tail to the high-energy side is a result of the ICH_2CN thermal energy distribution.

TABLE 2: Measured Onsets for ICH_2CN Photoionization^a

products	0 K energy (eV)
$\text{ICH}_2\text{CN}^{+\bullet}$	IE = 10.145 ± 0.010
$\text{CH}_2\text{CN}^{+\bullet} + \text{I}^{\bullet}$	DP ₀ = 12.188 ± 0.005
$\text{I}^{+\bullet} + \text{CH}_2\text{CN}^{\bullet}$	DP ₀ = 12.345 ± 0.010

^a DP₀ is the dissociative photoionization threshold at 0 K.

the detection of threshold electrons. The latter two factors are obtained directly from a threshold photoelectron spectrum of a simple molecule such as NO or C_2H_2 , which have large vibrational energy spacing between $\nu = 0$ and $\nu = 1$. A function was developed to account for these two factors and then convoluted with the thermal energy distribution of ICH_2CN . The form of the convoluted function is shown in Figure 4. The long tail to the left is associated with the “hot electron tail” that results from our inability to suppress the collection of all energetic electrons. The tail to the right is due to the thermal energy distribution. The only adjustable parameters in fitting the TOF distributions are the barrier heights for the formation of $^+\text{CH}_2\text{CN}$ and $\text{I}^{+\bullet}$, and the vibrational frequencies of the transition states for these two channels. The fits are indicated by the solid lines passing through the data in Figures 2 and 3. The 0 K onsets for the two dissociation limits are shown as dashed vertical lines in the breakdown diagram (Figure 3) and are listed in Table 2.

Figure 5 shows the dissociation rates calculated with the RRKM theory using the vibrational frequencies in Table 1. The molecular ion frequencies were those obtained from the ab initio calculations, while the transition state frequencies were adjusted to fit the data. The ΔS^{\ddagger} values shown in Figure 5 (16.7 and 20.8 J/(mol·K)) are both positive which indicate that these reactions proceed via loose transition states. This is characteristic of a simple bond-breaking step in the transition state. The loose transition state frequencies were generated by lowering some of the low frequencies until a good fit with the data was obtained.

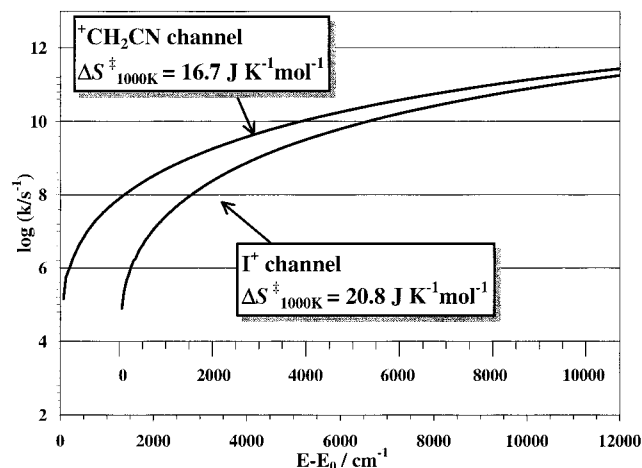


Figure 5. RRRM rate constants used to fit the breakdown diagram and the TOF distributions. The indicated ΔS^\ddagger values for both channels are positive and show that the dissociation is a simple bond-breaking step rather than an isomerization or rearrangement.

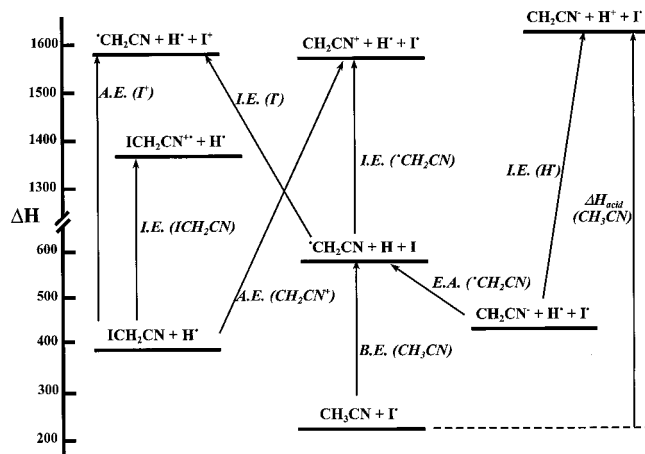


Figure 6. Energetics of the $\text{CH}_2\text{CN}/\text{I}/\text{H}$ system. The dashed vertical lines show the various experimentally measured transition energies and their relation to each other.

Thermochemistry

The usual approach to determining the heat of formation of the $^+\text{CH}_2\text{CN}$ ion from data such as are presented here is to use the heat of formation of the parent molecule, ICH_2CN . However, this heat of formation is not known experimentally. As was suggested in the Introduction, the heat of formation of the ICH_2CN molecule is at the heart of the discrepancies noted by Mayer and Radom.² Thus, we begin the cycle at a different point. The heat of formation of the $\bullet\text{CH}_2\text{CN}$ radical can be determined from the negative ion cycle. This same heat of formation can also be derived from neutral kinetics measurements of bond dissociation energies, as well as dissociative ionization studies that form this radical as product. We will then use our measurement of the $\bullet\text{CH}_2\text{CN}$ ionization energy to determine the heat of formation of the $^+\text{CH}_2\text{CN}$ ion. With this in hand, we can derive a heat of formation of the parent molecule, ICH_2CN . In this process we will also provide evidence that the structure of $\text{C}_2\text{H}_2\text{N}^+$ is the “linear” one. The relationships among these various quantities are shown in Figure 6.

A. $\Delta_f H^\circ(\text{CH}_3\text{CN})$, $\Delta H^\circ_{\text{acidity}}(\text{CH}_3\text{CN})$, $\text{EA}(\bullet\text{CH}_2\text{CN})$, and $\Delta_f H^\circ(\bullet\text{CH}_2\text{CN})$. We begin with the data that seem well established, some of which are listed in Table 3. These include the heat of formation of CH_3CN , which was measured by An and Mansson¹⁸ from its heat of combustion. This value is listed

TABLE 3: Experimental Heats of Formation of Various I, CH_nCN , and ICH_2CN Species (kJ/mol)^a

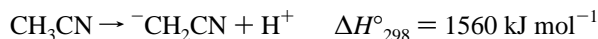
species	$\Delta_f H^\circ_{298\text{K}}$	$\Delta_f H^\circ_{0\text{K}}$	$H^\circ_{298\text{K}} - H^\circ_{0\text{K}}$	other 298 K values
I^\bullet	106.84 ^b	107.24 ^b	6.20 ^b	
I^+	1115.22 ^b	1115.63 ^b	6.20 ^b	
$\bullet\text{CH}_2\text{CN}$	252.6 ± 4^c	255.2 ± 4^c	12.3 ^d	245, ^e 243, ^f 243 \pm 13 ^g
$^+\text{CH}_2\text{CN}$	1245.9 ± 4^g	1248.4 ± 4^g	12.4 ^d	
$^-\text{CH}_2\text{CN}$	104.0 ± 4^c	106.4 ± 4^c	12.5 ^h	
ICH_2CN	172.5 ⁱ	179.7 ⁱ	14.3 ^d	
$\text{ICH}_2\text{CN}^{*+}$	1152.1 ± 4^i	1158.5 ± 4^i	15.1 ^d	
CH_3CN	74.0 ± 0.3^j	81.0 ± 0.4^k	12.1 ^j	

^a Heat capacity of an electron was treated as 0.0 kJ mol⁻¹ for all ion $\Delta_f H^\circ_{298\text{K}}$ values. 6.2 kJ/mol should be added to each ion heat of formation to conform to the JANAF standard. ^b From Wagman et al. (ref 29), but see note a. ^c Based on our analysis of the negative ion cycle. ^d Based on our ab initio calculations of the vibrational frequencies. ^e From Lifshitz et al. (ref 25). ^f From Trentwith (ref 26). ^g From Holmes et al. (ref 10). ^h Based on measured frequencies from Moran et al. (ref 20). ⁱ Derived on the basis of this work. ^j From An and Mansson (ref 18). ^k Based on measured vibrational frequencies reported by Shimanouchi (ref 19).

in Table 3 along with its 0 K analogue of 81.0 ± 0.4 kJ mol⁻¹. The 0 K value was determined by using $H^\circ_{298} - H^\circ_0 = 12.1$ kJ mol⁻¹ that was calculated with experimental vibrational frequencies listed in Shimanouchi.¹⁹

The second experimental measurement that is well established is the electron affinity (EA) of the $\bullet\text{CH}_2\text{CN}$ radical which was determined by Moran et al.²⁰ from the photoelectron spectrum of $^-\text{CH}_2\text{CN}$. A sharp 0–0 transition was observed from which they derived an $\text{EA}(\bullet\text{CH}_2\text{CN}) = 1.543 \pm 0.014$ eV. A simulation of the vibrational structure with ab initio calculated vibrational frequencies also confirmed that the structure of the negative ion was indeed $^-\text{CH}_2\text{CN}$. In addition, this structure is by far the most stable among the following: CH_2CN , CH_2NC , and cyclo- CHCHN .²

A final value that seems very well established is the 298 K acidity ($\Delta H^\circ_{\text{acidity}}$) of the CH_3CN molecule. The acidity is defined as the enthalpy change for the following reaction:



This was measured by Bartmess et al.²¹ through proton transfer equilibria between several gas phase acids to be 1524.6 kJ mol⁻¹. The old scale was later shifted as better absolute acidities became available. The new and accepted value is 1560 ± 11 kJ mol⁻¹,²² a number that has recently been confirmed by Matimba et al.²³ who found an acidity of 1559 ± 8 kJ mol⁻¹. Because the agreement is so good, it is tempting to lower the error bars to perhaps 4 kJ mol⁻¹. The error in these measurements appears to be the limiting factor in determining the derived values which follow. The fact that the $^-\text{CH}_2\text{CN}$ anion is so stable means that the structure of the anion produced from acetonitrile is not in question.

By combining the $\Delta_f H^\circ$ (CH_3CN), the $\Delta H^\circ_{\text{acidity}}$ (CH_3CN) and the $\text{EA}(\bullet\text{CH}_2\text{CN})$, we can derive a value for the heat of formation of the $\bullet\text{CH}_2\text{CN}$ radical. Because the EA measurement is a spectroscopic determination, it refers to the 0–0 transition and is thus a 0 K value. By using the 0 K heat of formation of acetonitrile, and converting the acidity to a 0 K value (1553.4 kJ mol⁻¹), we arrive at a 0 K heat of formation of the $\bullet\text{CH}_2\text{CN}$ radical of 255.2 ± 4 kJ mol⁻¹. This value is about 10 kJ mol⁻¹ higher than the one recommended by Berkowitz et al.¹ This is because they used an older and less reliable value²⁴ for the heat of formation of CH_3CN . The error in our derived value for the

$\bullet\text{CH}_2\text{CN}$ heat of formation is determined by the error in the CH_3CN acidity.

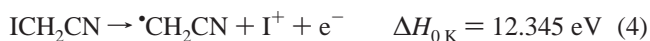
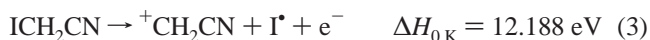
There are other measurements of the $\bullet\text{CH}_2\text{CN}$ heat of formation determined from the dissociation rate measurements of acetonitrile and related compounds. Lifshitz et al.²⁵ investigated the shock tube pyrolysis of acetonitrile and derived a C–H bond energy of 389 kJ mol^{-1} from which one calculates a 298 K heat of formation of the $\bullet\text{CH}_2\text{CN}$ radical of 245 kJ mol^{-1} . This is about 8 kJ mol^{-1} lower than our derived value based on the negative ion cycle (see Table 3). In high-pressure pyrolysis studies, numerous reactions intervene, of which only the first one is the simple C–H bond rupture. Subsequent bimolecular reactions such as $\bullet\text{CH}_3 + \text{CH}_3\text{CN} \rightarrow \text{CH}_4 + \bullet\text{CH}_2\text{CN}$, deplete the starting material. Thus, the interpretation of the activation energy of the overall reaction rate depends strongly on the assumed mechanism.

Another determination of the $\bullet\text{CH}_2\text{CN}$ heat of formation is from the very low pressure pyrolysis (VLPP) of propionitrile which yields $\text{CH}_3\bullet$ and $\bullet\text{CH}_2\text{CN}$. This method avoids the complications due to side and sequential reactions that sometimes confuse the analysis of high-pressure data. From the assumed heats of formation of the starting material, $\text{CH}_3\text{CH}_2\text{CN}$, and the methyl radical heat of formation, Trenwith²⁶ derived a 298 K $\bullet\text{CH}_2\text{CN}$ heat of formation of $242.7 \text{ kJ mol}^{-1}$. This value is 10 kJ mol^{-1} lower than the value derived on the basis of the negative ion cycle. However, the heat of formation of the propionitrile is perhaps the weak link in this method. The same group who published a value of the CH_3CN heat of formation that was 10 kJ mol^{-1} too low, also produced the propionitrile heat of formation of 52 kJ mol^{-1} .²⁴ Is this perhaps low as well? Still, the fact that the Trenwith and Lifshitz et al. values agree with each other lends some credibility to this lower $\bullet\text{CH}_2\text{CN}$ heat of formation.

A final quasi-experimental value for the heat of formation of the $\bullet\text{CH}_2\text{CN}$ radical was reported by Holmes et al.¹⁰ who produced this radical by electron impact ionization of $\text{HOCH}_2\text{CH}_2\text{CN}$ and $\text{CH}_3\text{OC(O)CH}_2\text{CN}$. They report an average value for the $\Delta_f H^\circ_{298}(\bullet\text{CH}_2\text{CN})$ of $243 \pm 13 \text{ kJ/mol}$. This is a quasi-experimental value because the heat of formation of the starting products are not known and had to be estimated by group additivity methods.

In summary, we conclude that the $\bullet\text{CH}_2\text{CN}$ heat of formation derived through the gas phase acidity of CH_3CN and the electron affinity of $\bullet\text{CH}_2\text{CN}$ is more reliable than ones derived through the pyrolysis of neutral species. This is because the ion cycle depends ultimately only on the heat of formation of acetonitrile and the experimental measurements of the gas phase acidity and the electron affinity. The interpretation of the latter two quantities for these species is relatively straightforward and does not depend on any questionable assumptions.

B. $\text{IE}(\bullet\text{CH}_2\text{CN})$, $\Delta_f H^\circ(+\text{CH}_2\text{CN})$, $\Delta_f H^\circ(\text{ICH}_2\text{CN})$, and $\Delta_f H^\circ(\text{ICH}_2\text{CN}^+)$. We next turn to our own data. The breakdown diagram in Figure 2 refers to the following two reactions:



By subtracting reaction 4 from reaction 3 and adding the ionization energy of I^\bullet to I^+ ($\text{IE} = 10.451 \text{ eV}$), we obtain the ionization energy of the $\bullet\text{CH}_2\text{CN}$ radical:



This value can be compared with recent direct measurements

TABLE 4: Comparison of Experimental and Theoretical Values at 298 K (in kJ mol^{-1})

quantity	experiments ^a	theory ^b	theory ^c	theory – expt (kJ mol^{-1})
$\text{BE}(\text{H}-\text{CH}_2\text{CN})$	396.8 ± 4	405 ± 3		8.2^b
$\text{IE}(\bullet\text{CH}_2\text{CN})$ (eV)	10.294 ± 0.005^d	10.25 ± 0.055^d	10.18^d	$-4.2,^b -11.0^c$
$\Delta_f H^\circ_{\text{acid}}(\text{CH}_3\text{CN})$	1560 ± 4	1568 ± 1		8.0^b
$\Delta_f H^\circ(\text{CH}_3\text{CN})$	74.0 ± 0.4	76.6 ± 2		2.6^b
$\Delta_f H^\circ(-\text{CH}_2\text{CN})$	104.0 ± 4	115.5 ± 2		11.5^b
$\Delta_f H^\circ(+\text{CH}_2\text{CN})$	252.6 ± 4	263.7 ± 2	246.5	$11.1,^b -6.1^c$
$\Delta_f H^\circ(+\text{CH}_2\text{CN})$	1245.9 ± 4	1252.8 ± 3.5	1229.1	$6.9,^b -16.8^c$
$\Delta_f H^\circ(\text{ICH}_2\text{CN})$	172.5 ± 4	153		-19.5^b

^a The experimental values are from various sources. See text. ^b From Mayer et al. (ref 2). ^c From Lau et al. (ref 5). ^d The ionization energy IE is a 0 K value.

of the ionization energy of this radical. Thorn et al.²⁷ determined the ionization energy by photoionization of the radical and reported a value of $10.28 \pm 0.01 \text{ eV}$, while Shea et al.²⁸ found an IE of $10.30 \pm 0.04 \text{ eV}$. Clearly our value agrees with these to within the experimental error. The error bars of $\pm 0.01 \text{ eV}$ can thus be assumed with considerable confidence.

The heat of formation of the $+\text{CH}_2\text{CN}$ ion now follows from this ionization energy and the heat of formation of the $\bullet\text{CH}_2\text{CN}$ radical. We obtain a $\Delta_f H^\circ_{0\text{K}}(+\text{CH}_2\text{CN}) = 1248.4 \pm 4 \text{ kJ mol}^{-1}$. Finally, we use the 0 K dissociative photoionization onset (DP₀) of 12.188 eV for the formation of $+\text{CH}_2\text{CN} + \text{I}$ to determine the heat of formation of the starting material, ICH_2CN . This leads to a $\Delta_f H^\circ_{0\text{K}}(\text{ICH}_2\text{CN}) = 179.7 \pm 4 \text{ kJ mol}^{-1}$ and a 298 K value of $172.5 \text{ kJ mol}^{-1}$. This value is considerably higher than the 152 kJ mol^{-1} determined by both group additivity and ab initio calculations. In fact, these data simply confirm the problem already noted by Mayer and Radom.²

What do our data tell us about the structure of the $\text{C}_2\text{H}_2\text{N}^+$ ion? Is it possible that the photoionization process is producing the lower energy cyclic form of this ion? Our data suggest otherwise. Because we observe both the production of $\bullet\text{CH}_2\text{CN}$ radical and the $+\text{CH}_2\text{CN}$ ion, and the difference in their onset energies (when combined with the $\text{IE}(\text{I})$) corresponds precisely to the ionization energy of the “linear” radical, it is impossible for another structure to have been produced. Also, since the “linear” geometry is the most stable structure for the free radical, it is certain that the $\bullet\text{CH}_2\text{CN}$ radical associated with the I^+ production is the “linear” form. Now if the cyclic form of the $\text{C}_2\text{H}_2\text{N}^+$ ion had been produced, then the ionization energy determined from our study would have been about 1 eV less than the observed energy of 10.294 eV . This difference is based on the energies of the neutral and ionic forms of the $\text{C}_2\text{H}_2\text{N}$ species as reported by Thorn et al.²⁷ This proof is in addition to the strong indication already noted by Mayer and Holmes.⁶ There are no other species involved in the cycle whose structure is in any doubt. Thus, it appears that the experimental evidence is overwhelmingly in favor of the ICH_2CN heat of formation listed in Table 3.

Comparison with Theoretical Values

The experimental values deemed by us to be the most accurate are compared with recent theoretical calculations^{2,5} in Table 4. The calculations of Mayer et al.² were carried out with the Gaussian 94 suite of programs¹⁷ and included two versions of the G2 approach,^{3,4} and two versions of the CBS programs. Their results in Table 4 are simple averages of the reported energies by the four methods, and the error bars reflect the variation among the methods used. Lau et al.⁵ reported just a single number from their G2 calculation with energy correction due to spin contamination. The first entries correspond to the

calculated energies of the indicated reactions, while the heat of formation of acetonitrile is determined from its atomization energy. The remaining heats of formation are then derived from this calculated value plus the energies associated with the indicated reactions. The differences between theory and experiment are thus not all independent values. For instance, in the case of the Mayer et al. results, the gas phase acidity and the bond energy of CH_3CN are high by about 8 kJ mol^{-1} and the heat of formation of the CH_3CN precursor is high by 2.6 kJ mol^{-1} . Hence, the derived heats of formation for $\bullet\text{CH}_2\text{CN}$ and $^-\text{CH}_2\text{CN}$ are high by the sum of these two, namely about 11 kJ mol^{-1} . It is interesting that the experimental results are in better agreement among each other than the theoretical calculations. The discrepancy between the calculated heats of formation of Mayer et al. and Lau et al. for $\bullet\text{CH}_2\text{CN}$ and $^+\text{CH}_2\text{CN}$ are particularly glaring. In both cases, the experimental results fall between the two sets of calculated values. Although the calculated ionization energy agrees quite well with the experimentally measured value, the discrepancy in the derived $^+\text{CH}_2\text{CN}$ heat of formation is compounded because it includes the discrepancy in the heat of formation of the $\bullet\text{CH}_2\text{CN}$ radical. The final entry is the heat of formation of the ICH_2CN which was calculated through the isodesmic reaction $\text{CH}_4 + \text{ICH}_2\text{CN} \rightarrow \text{CH}_3\text{I} + \text{CH}_3\text{CN}$ in which the numbers of like bonds is conserved (e.g., each side has six C–H bonds). The discrepancy here is $-19.5 \text{ kJ mol}^{-1}$.

In summary, the agreement among the experimental data is reasonably good, the largest discrepancy being the heat of formation of the $\bullet\text{CH}_2\text{CN}$ in which the ion cycle suggests a value that is 10 kJ/mol higher than the value from neutral kinetic measurements. On the other hand, the disagreement among the theoretical results is disturbing and the agreement of either set with experiment is less than desirable. While the agreement between theory and experiment is not superb, it is not unreasonable except for the case of iodoacetonitrile.

Conclusions

We have measured accurate onsets for the dissociative ionization of iodoacetonitrile to produce $^+\text{CH}_2\text{CN} + \text{I}^\bullet$ and $\bullet\text{CH}_2\text{CN} + \text{I}^+$. From these data we conclude that the structure of the $^+\text{CH}_2\text{CN}$ ion is the "linear" one. In combination with accurate measurements of the CH_3CN heat of formation, the gas phase acidity of acetonitrile, and the electron affinity of the $\bullet\text{CH}_2\text{CN}$ radical, we conclude that the 298 K heat of formation of the ICH_2CN molecule is $172.5 \pm 4 \text{ kJ mol}^{-1}$. This result is nearly 20 kJ mol^{-1} higher than the results from high-level ab initio calculations.

Acknowledgment. We thank the U.S. Department of Energy for a grant that supports this work. R.L. thanks the Natural Sciences and Engineering Council of Canada (NSERC) for a Postdoctoral Fellowship, and B.S. thanks the ELTE Peregrinatio and SOROS Foundations of Hungary for partial support of his stay in Chapel Hill.

References and Notes

- (1) Berkowitz, J.; Ellison, G. B.; Gutman, D. *J. Phys. Chem.* **1994**, *98*, 2744–2765.
- (2) Mayer, P. M.; Taylor, M. S.; Wong, M. W.; Radom, L. *J. Phys. Chem. A* **1998**, *102*, 7074–7080.
- (3) Curtiss, L. A.; Raghavachari, K.; Trucks, G. W.; Pople, J. A. *J. Chem. Phys.* **1991**, *94*, 7221–7230.
- (4) Curtiss, L. A.; Raghavachari, K.; Pople, J. A. *J. Chem. Phys.* **1993**, *98*, 1293–1298.
- (5) Lau, K. C.; Li, W. K.; Ng, C. Y.; Chiu, S. W. *J. Phys. Chem. A* **1999**, *103*, 3330–3335.
- (6) Holmes, J. L.; Mayer, P. M. *J. Phys. Chem.* **1995**, *99*, 1366–1370.
- (7) Mayer, P. M.; Baer, T. *J. Phys. Chem.* **1996**, *100*, 14949–14957.
- (8) Mazzyar, O. A.; Baer, T. *Int. J. Mass Spectrom. Ion. Processes* **1999**, *185*, 165–177.
- (9) Lafleur, R.; Baer, T., unpublished results, 1999.
- (10) Holmes, J. L.; Lossing, F. P.; Mayer, P. M. *Chem. Phys. Lett.* **1993**, *212*, 134–140.
- (11) Lifshitz, C. *Mass Spectrom. Rev.* **1982**, *1*, 309–348.
- (12) Baer, T. *Adv. Chem. Phys.* **1986**, *64*, 111–202.
- (13) Baer, T.; Booze, J. A.; Weitzel, K. M. In *Vacuum ultraviolet photoionization and photodissociation of molecules and clusters*; Ng, C. Y., Ed.; World Scientific: Singapore, 1991; pp 259–298.
- (14) Mazzyar, O. A.; Baer, T. *Chem. Phys. Lett.* **1998**, *288*, 327–332.
- (15) Wiley, W. C.; McLaren, I. H. *Rev. Sci. Instrum.* **1955**, *26*, 1150–1157.
- (16) Baer, T.; Hase, W. L. *Unimolecular Reaction Dynamics: Theory and Experiments*; Oxford University Press: New York, 1996.
- (17) Frisch, M. J.; Trucks, G. W.; Schlegel, H. B.; Gill, P. M. W.; Johnson, B. G.; Robb, M. A.; Cheeseman, J. R.; Keith, T. A.; Petersson, G. A.; Montgomery, J. A.; Raghavachari, K.; Al-Laham, M. A.; Zakrzewski, V. G.; Ortiz, J. V.; Foresman, J. B.; Cioslowski, J.; Stefanov, B. B.; Nanayakkara, A.; Challacombe, M.; Peng, C. Y.; Ayala, P. Y.; Chen, W.; Wong, M. W.; Andres, J. L.; Replogle, E. S.; Gomperts, R.; Martin, R. L.; Fox, D. J.; Binkley, J. S.; Defrees, D. J.; Baker, J.; Stewart, J. P.; Head-Gordon, M.; Gonzalez, C.; Pople, J. A. *GAUSSIAN 94*, Revision C.3; Gaussian Inc.: Pittsburgh, PA, 1995.
- (18) An, X. W.; Mansson, M. *J. Chem. Thermodyn.* **1983**, *15*, 287–293.
- (19) Shimanouchi, T. *Tables of Molecular Vibrational Frequencies*; Natl. Stand. Ref. Data. Ser. (NBS) No. 39; U.S. Government Printing Office: Washington, DC, 1972.
- (20) Moran, S.; Ellis, H. B., Jr.; Defrees, D. J.; McLean, A. D.; Ellison, G. B. *J. Am. Chem. Soc.* **1987**, *109*, 5996–6003.
- (21) Bartmess, J. E.; Scott, J. A.; McIver, R. T., Jr. *J. Chem. Soc.* **1979**, *101*, 6056–6063.
- (22) Lias, S. G.; Bartmess, J. E.; Liebman, J. F.; Holmes, J. L.; Levin, R. D.; Mallard, W. G. Gas-Phase Ion and Neutral Thermochemistry; *J. Phys. Chem. Ref. Data* Vol 17, Suppl. 1; NSRDS, U.S. Government Printing Office: Washington, DC, 1988.
- (23) Matimba, H. E. K.; Crabbendam, A. M.; Ingemann, S.; Nibbering, N. M. M. *Int. J. Mass Spectrom. Ion. Processes* **1992**, *114*, 85–97.
- (24) Hall, H. K., Jr.; Baldt, J. H. *J. Am. Chem. Soc.* **1971**, *93*, 140–145.
- (25) Lifshitz, A.; Moran, A.; Bidani, S. *Int. J. Chem. Kinet.* **1987**, *19*, 61–79.
- (26) Trenwith, A. B. *J. Chem. Soc., Faraday Trans. 1* **1983**, *79*, 2755–2764.
- (27) Thorn, R. P., Jr.; Monks, P. S.; Stief, L. J.; Kuo, S. C.; Zhang, Z.; Ross, S. K.; Klemm, R. B. *J. Phys. Chem. A* **1998**, *102*, 846–851.
- (28) Shea, D. A.; Steenvoorden, R. J. J. M.; Chen, P. *J. Phys. Chem. A* **1997**, *101*, 9728–9731.
- (29) Wagman, D. D.; Evans, W. H. E.; Parker, V. B.; Schum, R. H.; Halow, I.; Mailey, S. M.; Churney, K. L.; Nuttall, R. L. The NBS Tables of Chemical Thermodynamic Properties; *J. Phys. Chem. Ref. Data* Vol. 11 Suppl. 2; NSRDS, U.S. Government Printing Office; Washington, DC, 1982.